Enhanced light harvesting of nitride-based nanopillars covered with ZnO using indium–tin oxide nanowhiskers

2014 Jpn. J. Appl. Phys. 53 04ER10

(http://iopscience.iop.org/1347-4065/53/4S/04ER10)

Japanese Journal of Applied Physics **53**, 04ER10 (2014) **REGULAR PAPER**
http://dx.doi.org/10.7567/JJAP.53.04ER10

Enhanced light harvesting of nitride-based nanopillars covered with ZnO using indium–tin oxide nanowhiskers

Lung-Hsing Hsu[1], Chien-Chung Lin[2*], Hsin-Ying Lee[3], Jhih-Kai Huang[4], Hau-Vei Han[4], Yu-Lin Tsai[4], Peichen Yu[4], Hao-Chung Kuo[4], and Ching-Ting Lee[5]

[1]*Institute of Lighting and Energy Photonics, College of Photonics, National Chiao Tung University, Tainan 71150, Taiwan*
[2]*Institute of Photonic Systems, College of Photonics, National Chiao Tung University, Tainan 71150, Taiwan*
[3]*Department of Photonics, National Cheng Kung University, Tainan 70101, Taiwan*
[4]*Department of Photonics and Institute of Electro-Optical Engineering, National Chiao Tung University, Hsinchu 30010, Taiwan*
[5]*Institute of Microelectronics, Department of Electrical Engineering, National Cheng Kung University, Tainan 70101, Taiwan*
E-mail: chienchunglin@faculty.nctu.edu.tw

Received September 24, 2013; revised November 13, 2013; accepted November 18, 2013; published online March 4, 2014

Nitride-based nanopillars were successfully fabricated by nanoimprint lithography. A nanowhisker of indium–tin oxide (ITO) deposited by on oblique evaporation method was investigated in nitride-based nanopillars and thin ZnO layers grown by atomic layer deposition (ALD). From the results of field-emission scanning electron microscopy (SEM) measurement, it was found that ITO whiskers grew on nitride-based nanopillars covered with ZnO. Moreover, from the results of UV–visible spectrophotometry and bidirectional reflectance distribution function (BRDF) measurements, it was found that this hybrid structure of ITO nanowhiskers above a ZnO medium enhanced the broadband and angle-independent antireflection in the range between 380 and 600 nm. We used the hybrid design of the ITO/ZnO structure to achieve the lowest reflectance value between 3.8 and 10.9% in a quantum well absorption range.

1. Introduction

Nowadays, the development of high-efficiency optoelectronic devices is considered as one of the crucial topics in visible light communication, integration of mobile telecommunication, human–computer interaction of room lighting[1)] and display, and photovoltaic devices.[2)] Among the materials adopted for solar cells, III–V alloys (such as GaAs and InP) are the forerunners at present as they hold the record of power conversion efficiency (PCE).[3)] GaN-based p–i–n diodes with luminescence covering the range from infrared to ultraviolet (0.7 to 6.2 eV) have been extensively applied in large full-color displays, short-haul optical communication, traffic and signal lights, backlight for liquid-crystal displays, and general-purpose light fixtures.[4)] Typically, a GaN-based epilayer is grown on a planar sapphire substrate by hetero-epitaxial techniques, such as metal–organic chemical vapor deposition (MOCVD).[5,6)] Recently, nanoscale epitaxial overgrowth[7)] has been found to be promising for enhancing the performance of nitride-based optoelectronic devices. Owing to the nanoscale pattern process[8–13)] and epitaxy, overgrowth of nanostructures not only improves crystal quality[14)] but also produces a scattering effect on the emitted photons, leading to a higher light extraction efficiency (LEE).[15)]

Recently, indium–tin oxide (ITO) and ZnO have emerged as promising choices of transparent conductive oxides (TCOs) for enhancing the external efficiency of devices owing to their low absorption in the visible spectrum, intermediate refractive indices, and good electronic conduction. Although traditional antireflective coating is successful in photovoltaic devices, the pursuit of a broadband and angle-independent antireflection remains strong.[16–19)] Recent studies have shown that antireflective nanostructures can be tailored for optimal light harvesting, regardless of photon wavelength, angle of incidence, and level of polarization.[20–23)] The light trapping effect and enhanced conversion efficiency in nanometer-scaled structures have also been demonstrated in thin-film and nanowire optoelectronic devices.[24–26)] Nevertheless, fabricating nanostructures on several material templates risk increases in scattering and surface recombination losses. Moreover, the technologies required to combine both micro- and nano-scale surface textures and the associated advantages are very essential. In addition, several studies have examined the uniformity issue of the application of nanometer-scaled pillars.[27,28)] Although the performance of the devices enhanced significantly, their pattern shapes were still random around the surface.

Previously, we reported about ITO whiskers and their use in light harvesting.[29)] In this study, uniform and periodic nanometer-scaled GaN-based p–i–n pillars were fabricated using the nanoimprint lithography (NIL) technique and the inductively coupled plasma (ICP-RIE) etching process. A ZnO thin film was grown to cover GaN-based p–i–n nanopillars and then ITO whiskers were deposited onto it. The field-emission scanning electron microscopy (SEM) measurement was accurate in detecting the appearance of this hybrid nanometer-scaled structure. Furthermore, the photoluminescence (PL) and broadband angle-independent reflection characteristics were measured to assess the optical impact of the hybrid TCO structure on nanopillars.

2. Experimental procedure

The nitride-based structures were grown on *c*-plane sapphire substrates by MOCVD with a rotating disk reactor (Veeco D180). On the bottom sapphire substrate, the epitaxial layers consist of a 30-nm-thick GaN nucleation layer grown at 525 °C, a 2-μm-thick undoped GaN layer grown at 1050 °C, a 2-μm-thick Si-doped n-type GaN layer grown at 1050 °C, followed by a 70-nm-thick active layer of five pairs of $In_{0.17}Ga_{0.83}N$/GaN multiple quantum wells (MQWs) consisting of a 2-nm-thick well and a 12-nm-thick barrier grown at 770 °C, and a 0.2-μm-thick Mg-doped p-type GaN layer grown at 1025 °C. After standard fabrication steps, we used NIL to generate nitride-based nanopillars (NPs). Two-dimensional square-lattice air-hole arrays with a lattice constant of 500 nm were formed by NIL techniques. The steps of the NIL process were described as follows: step 1 — generating a photonic quasi-crystal (PQC) patterned mold of an inter-

mediate polymer stamp (IPS) from a Ni master stamp. We chose a 12-fold PQC pattern owing to a more enhanced surface emission.[30] This pattern was obtained from photonic crystals (PhCs) with a dodecagonal symmetric quasi-crystal lattice, as opposed to regular PhCs with a triangular lattice and an 8-fold PQC.[31] The NIL system was preheated at a temperature of 150 °C under a pressure of 30 bar for about 5 min. In step 2, a 100-nm-thick polymer layer was spin-coated on a 200-nm-thick SiO_2/GaN LED wafer surface, the SiO_2 layer of which was grown by plasma-enhanced chemical vapor deposition (PECVD). The temperature and pressure of the NIL system were then changed to 65 °C and 40 bar to proceed to step 3. Step 3 was a second imprint using the IPS as a single useful template to transfer the PQC pattern onto the dried polymer film in a simultaneous thermal and UV process (STU). By UV irradiation for 10 s, the PQC pattern was transferred to the polymer layer on the surface of the LED wafer. In step 4, the NIL system was cooled to room temperature to release the IPS from the LED wafer. In step 5, we use an inductively coupled plasma reactive ion etching (ICP-RIE) system with CF_4 plasma to remove the residual polymer layer and transfer the pattern onto the SiO_2 layer. The ICP-RIE system used the reactive gas CHF_3 and O_2 with an RF power of 250 W and a chamber pressure of 4 Pa. After the NIL process, the atomic layer deposition (ALD) technique was employed to grow a 120-nm-thick ZnO thin film for covering nitride-based nanopillars at a temperature of 200 °C. Finally, ITO nanowhiskers (NWs) were deposited at an oblique angle by electron beam evaporation. For comparison, two samples were prepared during the NW deposition: one is with conventional flat devices and the other is with NPs covered with ZnO on the surface, as shown in Fig. 1.

To fabricate the novel structure of hybrid ITO NWs/ZnO, as transparent conductive oxide layers, a higher transparency and a lower resistivity are crucial to the efficiency of optoelectronic devices. The resistivity and transparency of ITO NWs are $\sim 2 \times 10^{-4}\,\Omega\,\mathrm{cm}$ and ~80 to 90%, respectively, and the average height of NWs on nitride-based structures is 1.2 μm. In addition, the height and diameter of NPs covered with ZnO are 920 and 550 nm, respectively. The spacing distance between NPs ranges between 50 and 320 nm. The SEM images of hybrid ITO NWs/ZnO on NPs are shown in Fig. 2.

3. Results and discussion

Six different structural combinations were fabricated for characterization: (1) NPs, (2) NPs covered with ZnO by ALD (ZnO + NPs), (3) NWs deposited onto NPs (NWs + NPs), (4) NWs deposited onto NPs covered with ZnO (NWs + ZnO + NPs), (5) NWs deposited onto conventional devices (NWs + flat), and (6) conventional devices (flat). Figure 3 shows that the PL spectral peak wavelength of InGaN/GaN (MQWs) at room temperature is ~455 nm. The photoluminescence was measured using the 325 nm line of a He–Cd laser (2 mW) as the excitation source. Four different samples were measured for their PL characteristics. The samples with only NPs and NWs + NPs showed a two-peak profile: one peak is for InGaN MQWs and the other peak (365 nm) is for bulk GaN. However, the GaN peak disappeared after ZnO was deposited onto the NPs, which can be explained by further absorption induced by ZnO.

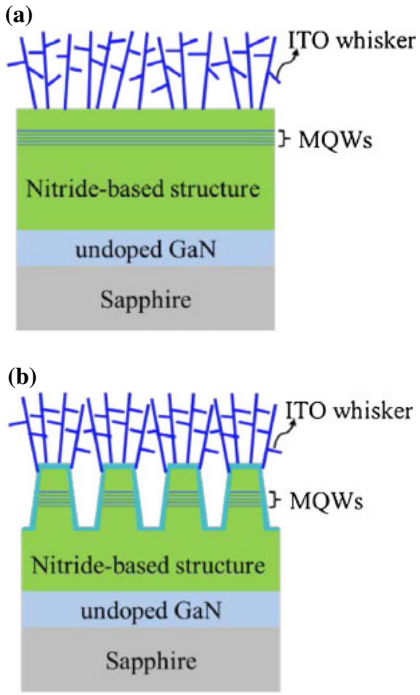

Fig. 1. (Color online) Schematic diagram: (a) NWs on conventional devices and (b) NWs on NPs covered with ZnO.

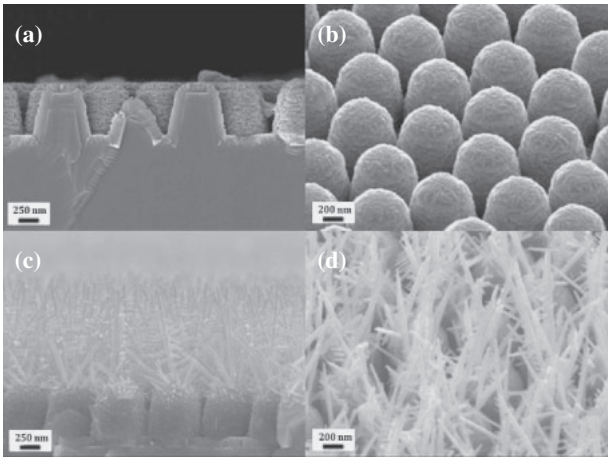

Fig. 2. SEM images for (a) cross section and (b) tilted image of NPs covered with ZnO; (c) cross section and (d) tilted image of NWs on NPs covered with ZnO.

Figure 4(a) shows the reflectance values of all structural combinations, namely, NPs, ZnO + NPs, NWs + NPs, NWs + ZnO + NPs, NWs + flat, and flat. Figure 4(b) shows the enhanced factor of light harvesting of NWs on different templates, NPs, and NPs covered with ZnO, compared with conventional devices. The enhanced factor (F_{enhanced}) of light harvesting is defined as

$$F_{\mathrm{enhanced}} = R_f/R_i, \tag{1}$$

where R_i is the reflectance of a structure and R_f is the reflectance of a conventional device. We found that the reflectance of the NW sample on NPs covered with ZnO is lower than those of the NP sample and the NP sample covered with ZnO, the correlated wavelength of which ranges

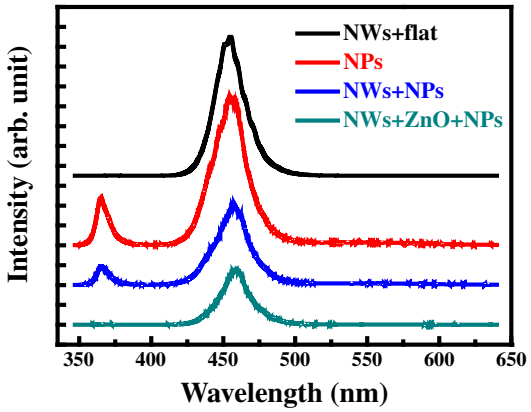

Fig. 3. (Color online) PL spectra for NPs, NWs on NPs, NWs on NPs covered with ZnO, and NWs on conventional devices.

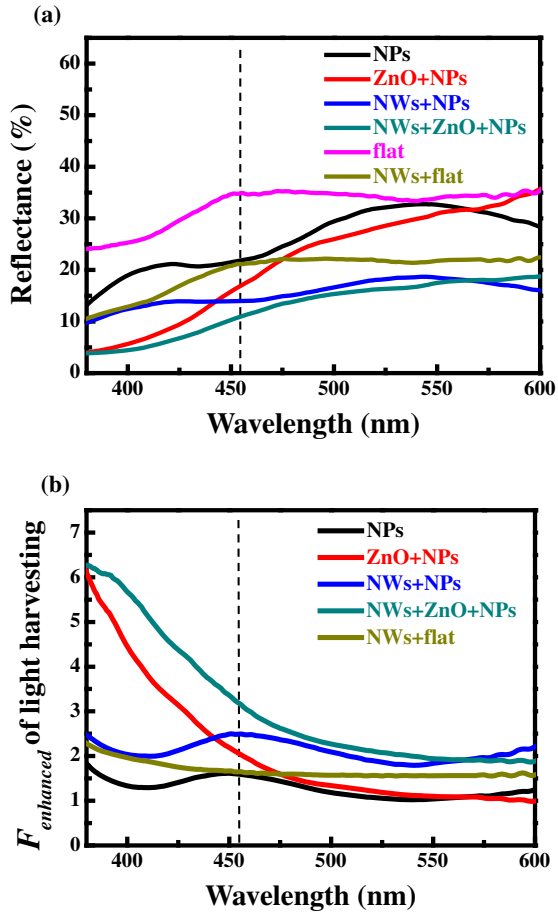

Fig. 4. (Color online) (a) Reflectance correlated wavelength of NWs on different templates, conventional devices, NPs, and NPs covered with ZnO. (b) Enhanced factor of light harvesting at correlated wavelength of NWs on different templates, NPs, and NPs covered with ZnO; the dotted line shows the factor at the wavelength of 455 nm.

from 380 to 562 nm. Among the test samples, the hybrid ITO NW/ZnO structure exhibited the lowest reflectance values between 3.8 and 10.9% in the wavelength range from 380 to 455 nm. Furthermore, the F_{enhanced} of the hybrid ITO NW/ZnO structure is higher than that of NWs on conventional devices. The F_{enhanced} of the hybrid ITO NW/ZnO structure reaches high values of 6.3 and 3.4 at wavelengths of

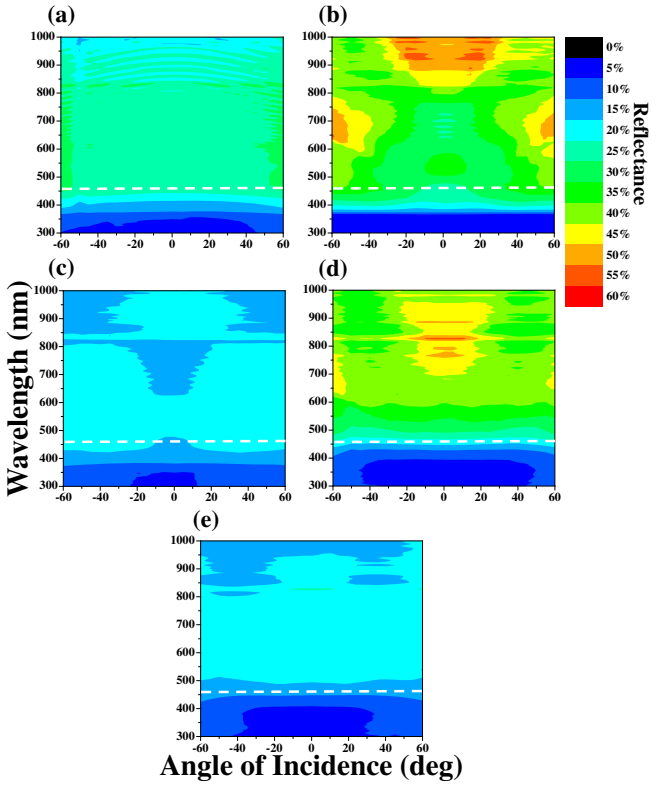

Fig. 5. (Color online) Measured angle-resolved reflectance spectra of (a) NWs on conventional devices, (b) NPs, (c) NWs on NPs, (d) NPs covered with ZnO, and (e) NWs on NPs covered with ZnO; the dotted line shows the factor at the wavelength of 455 nm.

380 and 455 nm, respectively. For wavelengths shorter than 442 nm, the reflectance of NPs + ZnO is lower than that of NWs + NPs. This is mainly caused by the fact that the uniform gradual change brought by the ZnO layer can perform better in terms of lowering the Fresnel reflection, similarly to that observed in the previously reported work[29] performed using the gradual refractive index theory. In contrast, all the nanowhiskers are standing on the top of the nanopillars, leaving some air gaps between the substrate and the nanopillars, and this may induce further refractive index disruption and leads to a higher reflectivity.

Figure 5 shows the measured angular reflectance spectra of NPs, NPs covered with ZnO, and NWs on different templates. The reflectance of the NPs remained low at small angles of incidence (AOIs), compared with those of the other samples. Nevertheless, the ITO NWs and ZnO deposited onto NPs were both effective in preserving the low reflectance at large angles of incidence. The low reflectance (3.4% of reflection or less) can be found from 300 to 1000 nm and from −60 to +60°. Large-area omnidirectional antireflective structures are very beneficial to photovoltaic devices. We demonstrated that NWs not only inhibit the broadband reflectivity at wavelengths up to 1000 nm for normal incidence but also maintain a low reflectance under various incident angles up to ±60°. In addition to NWs, the ZnO thin film also restrained the broadband reflectivity at wavelengths up to 455 nm to improve the absorption of MQWs through the illustrations in Figs. 5(b) and 5(d). The results reveal that the NW sample on NPs covered with ZnO showed the best

antireflection characteristics over the entire spectrum from 300 to 1000 nm and an AOI up to 60 degrees.

4. Conclusions

We fabricated a hybrid ITO NW structure onto nitride-based NPs covered with ZnO that enhanced antireflection and found that the enhanced factor of light harvesting is higher than that of NWs on conventional devices in the range between 380 and 600 nm. This reveals that a hybrid ITO NW/ZnO structure is feasible for improving the light trapping efficiency of optoelectronic devices.

Acknowledgments

The authors would like to thank the Department of Electrical Engineering and Institute of Microelectronics, National Cheng Kung University, for the technical support. This work was sponsored by the National Science Council of Taiwan through contract numbers NSC101-2221-E-009-046-MY3, NSC 102-2120-M-110-005, and NSC 102-3113-E-005-001.

1) T. Fujii, Y. Gao, R. Sharma, E. L. Hu, S. P. DenBaars, and S. Nakamura, Appl. Phys. Lett. **84**, 855 (2004).
2) C. J. Neufeld, N. G. Toledo, S. C. Cruz, M. Iza, S. P. DenBaars, and U. K. Mishra, Appl. Phys. Lett. **93**, 143502 (2008).
3) P. Yu, C.-H. Chang, C.-H. Chiu, C.-S. Yang, J.-C. Yu, H.-C. Kuo, S.-H. Hsu, and Y.-C. Chang, Adv. Mater. **21**, 1618 (2009).
4) Y. Narukawa, I. Niki, K. Izuno, M. Yamada, Y. Murazaki, and T. Mukai, Jpn. J. Appl. Phys. **41**, L371 (2002).
5) E. F. Schubert, *Light-Emitting Diodes* (Cambridge University Press, Cambridge, U.K., 2003) 2nd ed., p. 21.
6) J. Han, M. H. Crawford, R. J. Shul, J. J. Figiel, M. Banas, L. Zhang, Y. K. Song, H. Zhou, and A. V. Nurmikko, Appl. Phys. Lett. **73**, 1688 (1998).
7) C. H. Chiu, Z.-Y. Li, C. L. Chao, M. H. Lo, H. C. Kuo, P. C. Yu, T. C. Lu, S. C. Wang, K. M. Lau, and S. J. Cheng, J. Cryst. Growth **310**, 5170 (2008).
8) Y. J. Lee, J. M. Hwang, T. C. Hsu, M. H. Hsieh, M. J. Jou, B. J. Lee, T. C. Lu, H. C. Kuo, and S. C. Wang, IEEE Photonics Technol. Lett. **18**, 1152 (2006).
9) Z. H. Feng, Y. D. Qi, Z. D. Lu, and K. M. Lau, J. Cryst. Growth **272**, 327 (2004).
10) T. V. Cuong, H. S. Cheong, H. G. Kim, H. Y. Kim, C.-H. Hong, E. K. Suh, H. K. Cho, and B. H. Kong, Appl. Phys. Lett. **90**, 131107 (2007).
11) H. Park, K.-J. Byeon, J.-J. Jang, O. Nam, and H. Lee, Microelectron. Eng. **88**, 3207 (2011).
12) H. Gao, F. Yan, Y. Zhang, J. Li, Y. Zeng, and G. Wang, J. Appl. Phys. **103**, 014314 (2008).
13) D. S. Wuu, W. K. Wang, K. S. Wen, S. C. Huang, S. H. Lin, R. H. Horng, Y. S. Yu, and M. H. Pan, J. Electrochem. Soc. **153**, G765 (2006).
14) T.-Y. Tang, C.-H. Lin, Y.-S. Chen, W.-Y. Shiao, W.-M. Chang, C.-H. Liao, K.-C. Shen, C.-C. Yang, M.-C. Hsu, J.-H. Yeh, and T.-C. Hsu, IEEE Trans. Electron Devices **57**, 71 (2010).
15) C. H. Kuo, L. C. Chang, C. W. Kuo, and G. C. Chi, IEEE Photonics Technol. Lett. **22**, 257 (2010).
16) P. Lalanne and G. M. Morris, Proc. SPIE **2776**, 300 (1996).
17) C. H. Chiu, P. Yu, H. C. Kuo, C. C. Chen, T. C. Lu, S. C. Wang, S. H. Hsu, Y. J. Cheng, and Y. C. Chang, Opt. Express **16**, 8748 (2008).
18) P.-C. Tseng, P. Yu, H.-C. Chen, Y.-L. Tsai, H.-W. Han, M.-A. Tsai, C.-H. Chang, and H.-C. Kuo, Sol. Energy Mater. Sol. Cells **95**, 2610 (2011).
19) H.-C. Chen, C.-C. Lin, H.-W. Han, Y.-L. Tsai, C.-H. Chang, H.-W. Wang, M.-A. Tsai, H.-C. Kuo, and P. Yu, Opt. Express **19**, A1141 (2011).
20) J.-Q. Xi, M. F. Schubert, J. K. Kim, E. F. Schubert, M. Chen, S.-Y. Lin, W. Liu, and J. A. Smart, Nat. Photonics **1**, 176 (2007).
21) C. H. Chiu, P. Yu, C. H. Chang, C. S. Yang, M. H. Hsu, H. C. Kuo, and M. A. Tsai, Opt. Express **17**, 21250 (2009).
22) C. H. Chang, P. Yu, and C. S. Yang, Appl. Phys. Lett. **94**, 051114 (2009).
23) Y. Kanamori, K. Hane, H. Sai, and H. Yugami, Appl. Phys. Lett. **78**, 142 (2001).
24) J. Zhu, C.-M. Hsu, Z. Yu, S. Fan, and Y. Cui, Nano Lett. **10**, 1979 (2010).
25) M. D. Kelzenberg, S. W. Boettcher, J. A. Petykiewicz, D. B. Turner-Evans, M. C. Putnam, E. L. Warren, J. M. Spurgeon, R. M. Briggs, N. S. Lewis, and H. A. Atwater, Nat. Mater. **9**, 368 (2010).
26) E. C. Garnett and P. Yang, J. Am. Chem. Soc. **130**, 9224 (2008).
27) Y. K. Su, J. J. Chen, C. L. Lin, S. M. Chen, W. L. Li, and C. C. Kao, J. Cryst. Growth **311**, 2973 (2009).
28) B.-J. Kim, M. A. Mastro, H. Jung, H.-Y. Kim, S. H. Kim, R. T. Holm, J. Hite, C. R. Eddy, Jr., J. Bang, and J. Kim, Thin Solid Films **516**, 7744 (2008).
29) C.-H. Chang, P. Yu, M.-H. Hsu, P.-C. Tseng, W.-L. Chang, W.-C. Sun, W.-C. Hsu, S.-H. Hsu, and Y.-C. Chang, Nanotechnology **22**, 095201 (2011).
30) C.-E. Lee, C.-F. Lai, Y.-C. Lee, H.-C. Kuo, T.-C. Lu, and S.-C. Wang, IEEE Photonics Technol. Lett. **21**, 331 (2009).
31) Z. S. Zhang, B. Zhang, J. Xu, K. Xu, Z. J. Yang, Z. X. Qin, T. J. Yu, and D. P. Yu, Appl. Phys. Lett. **88**, 171103 (2006).